Thermal-induced evolution of secondary phases in Cr–Mo–V low alloy steels

J. JANOVEC*
Slovak University of Technology, Faculty of Materials Science and Technology, Department of Materials Engineering, Bottova 23, 917 24 Trnava, Slovakia
E-mail: jozef.janovec@stuba.sk

M. SVOBODA, A. KROUPA
Academy of Sciences of the Czech Republic, Institute of Physics of Materials, Žižkova 22, 616 62 Brno, Czech Republic

A. VÝROSTKOVÁ
Slovak Academy of Sciences, Institute of Materials Research, Watsonova 47, 043 53 Košice, Slovakia

Published online: 12 April 2006

Four low alloy steels with different contents of molybdenum and vanadium were investigated. The steels were annealed at 773, 793, 853, 873, 933, 973, and 993 K for 500, 1000, 3000, and 10000 h. Techniques of transmission electron microscopy and thermodynamic calculations (ThermoCalc) were used to characterise influence of the steel bulk composition and the annealing conditions on evolution of carbides M_3C, M_2C, M_7C_3, $M_{23}C_6$, M_6C, and MC (M = metallic element). Changes in structure types and metal compositions of the carbides were characterised in detail. The work was done with the intention to obtain more information about the secondary phase evolution in low alloy steels used in energy industries.

1. Introduction

The claim to the safety, environmental, and economical operation of power plants has evoked the research and development of advanced materials for energy industries including low alloy steels. Considerable attention has been recently attributed to the investigation of secondary phases as M_3C, M_7C_3, $M_{23}C_6$, M_2C (M_2X), M_6C (M_6X), and MC (MX), where M = Fe, Cr, Mo, V, etc. and X = C + N [1–5]. The M_3C, M_7C_3 (both of the orthorhombic crystal lattice), and $M_{23}C_6$ (f.c.c. crystal lattice) can be characterised as Cr-Fe-rich carbides [1, 6–8]. Other three secondary phases can alternate between the carbidic (M_2C, M_6C, MC) and the carbonitridic (M_2X, M_6X, MX) modifications [9, 10]. Even if metal compositions of the secondary phases are dependent on bulk compositions of steels, the hexagonal M_2C (M_2X) contains mainly molybdenum, tungsten, and/or chromium [11]. Molybdenum, tungsten, and/or iron are usually present in the massive M_6C (M_6X) particles [12, 13]. Metals showing a high enough affinity to carbon and/or nitrogen (V, Ti, Nb, Zr) occur usually in dispersive MC (MX) particles [14]. Next to the above mentioned secondary phases, the orthorombic Cr_3C_2 was predicted by Goldschmidt [15]. However, this carbide was not experimentally confirmed in low alloy steels [16]. The ξ-carbide predicted for molybdenum, tungsten, and/or chromium containing steels shows the analogy to M_3C [17]. The hexagonal ε-carbide, observed mostly in the self-tempered martensite, transforms into M_3C in early stages of tempering [4].

For characterisation of the secondary phase particles, exact techniques of transmission electron microscopy (TEM), electron, X-ray, and neutron diffraction, energy- (EDX) and wave-dispersion (WDX) X-ray spectroscopy, Mössbauer spectroscopy, etc. are used [18–21]. However, the steel can be exerted in energy industries, when all its components, inclusive of the secondary phase particles, show the sufficient microstructure stability. In other words, the parameters measured experimentally should be in reasonable agreement with the equilibrium values. Unfortunately, only small part of the experimental results can be considered as being close to the equilibrium state, because for reaching the equilibrium

*Author to whom all correspondence should be addressed.
0022-2461
DOI: 10.1007/s10853-006-6744-7

conditions an extremely long annealing is necessary [22]. A partial solution of this problem consists in the use of the Calphad method (the **cal**culation of **pha**se **d**iagrams on the basis of thermodynamic properties of individual phases) that makes possible a more effective exploitation of the available experimental data to predict phase equilibria [23]. The thermodynamic database programs (e.g. ThermoCalc, MTDATA, Dictra) together with the reliable databases are useful tools for the material characterisation, when they are used complementary to the experimental findings [24–26].

In this work, secondary phases were investigated in four low alloy steels. The steels were isothermally exposed at temperatures between 700 and 1000 K for long enough periods. To characterise the stability and metal compositions of secondary phases both experimental measurements and thermodynamic calculations were used. The work was done with the intention to obtain more information about the evolution of secondary phases in the investigated steels at temperatures corresponding to service conditions in power plants.

2. Experimental

The steels (Table I) were melted in a vacuum furnace, forged to rods, austenitised at 1523 K for 0.75 h, and quenched into aques solution of potassium hydroxide. The quenched samples were annealed at 773, 793, 853, 873, 933, 973 and 993 K for 500, 1000, 3000 and 10000 h. Particles of secondary phases were extracted into carbon replicas and identified with a TEM Philips CM12 working at 120 kV. Selected area electron diffraction (SAD) and energy dispersive X-ray spectroscopy (EDX) were used for characterisation of the particles. The identification procedure is documented in Figs 1a (it shows morphology of the analysed particle and the corresponding EDX-spectrum) and 1b (selected area diffraction pattern). Metal compositions of the analysed particles were determined from EDX-spectra with evaluation method, adjusted for thin samples. No corrections for absorption or fluorescence were made, because the average thickness of the particles was below 200 nm.

Complex carbides in low alloy steels can be characterised as multicomponent systems containing more metallic elements. However, some elements do not play any important role in influencing the carbide properties, because of their very limited contents. With intention to do the work easy to survey, atomic and weight concentrations of the two dominant metallic elements were divided,

TABLE I. Chemical compositions of investigated steels; mass contents of elements are given in %

Steel	C	Mn	Si	Cr	V	Mo	P	S	Fe
1	0.09	0.66	0.32	2.40	0.02	0.70	0.011	0.006	bal.
2	0.10	0.66	0.35	2.55	0.12	0.73	0.015	0.005	bal.
3	0.10	0.67	0.27	2.62	0.32	0.70	0.014	0.007	bal.
4	0.12	0.71	0.34	2.57	0.34	0.95	0.015	0.018	bal.

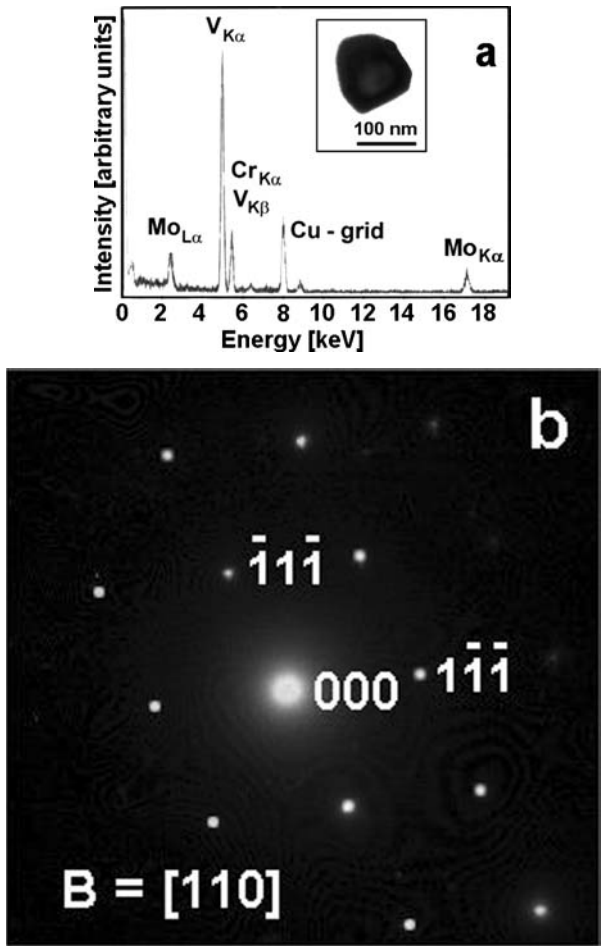

Figure 1 Procedure used in carbide identification: (a) morphology of the analysed particle (TEM-image is documented in the small window) and corresponding EDX spectrum, (b) selected area electron diffraction pattern. The data revealed from the diffraction pattern (f.c.c. crystal structure with the lattice parameter $a = 0.422$ nm) and from the EDX-spectrum (peaks of $Mo_{L\alpha}$,$V_{K\alpha}$,$V_{K\beta}Cr_{K\alpha}$,and $Mo_{K\alpha}$) confirmed the analysed particle is of MC-type.

to obtain ratios well characterising metallic parts of the particular carbides. For carbides M_3C, M_7C_3, and $M_{23}C_6$, the Cr/Fe ratio was chosen as the most appropriate parameter. Similarly, the Mo/Cr, Mo/Fe and V/Mo ratios were considered to be the most illustrative for the M_2C, M_6C and MC carbides, respectively. The average values of the above ratios were calculated from 10 experimental measurements, at least.

3. Thermodynamic calculations

The thermodynamic calculations for systems corresponding to the steels were done in the temperature range 750–1000 K. In the calculations, the ThermoCalc program [24, 26] and the non-commercial database Steel16 [27] were used. The attention was paid to prediction of both the phase equilibria and the chemical compositions of equilibrium phases. In the calculation procedure, the total Gibbs energy of the system consisting of contributions of individual phases is minimized at constant temperature

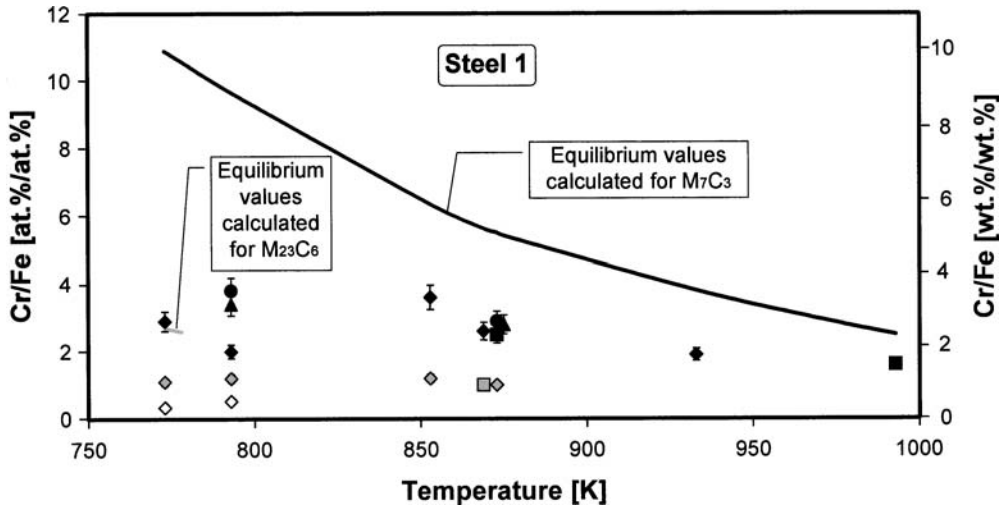

Figure 2 Experimental (points) and calculated equilibrium values (curves) of the Cr/Fe ratio as a function of temperature; plotted for steel 1. Meanings of the non-labelled symbols follow from Table VII.

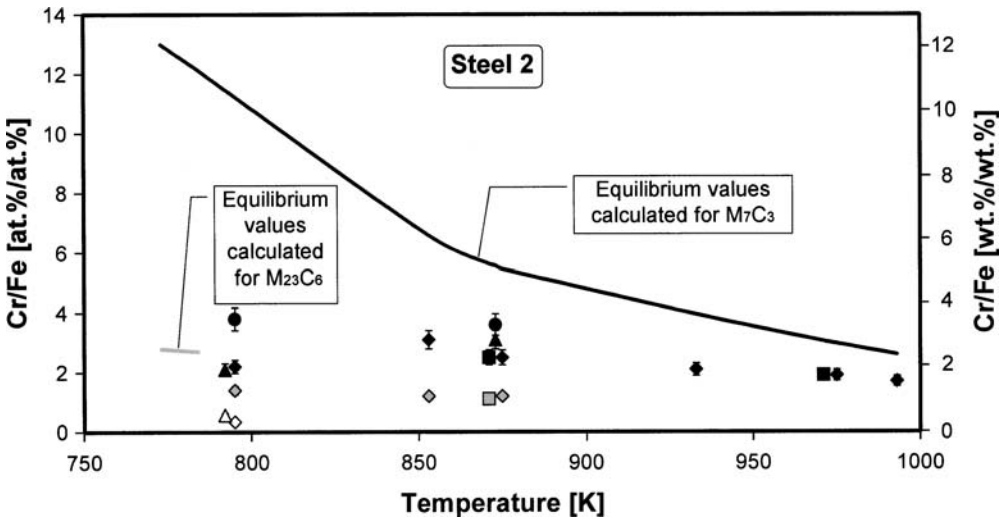

Figure 3 Experimental (points) and calculated equilibrium values (curves) of the Cr/Fe ratio as a function of temperature; plotted for steel 2. Meanings of the non-labelled symbols follow from Table VII.

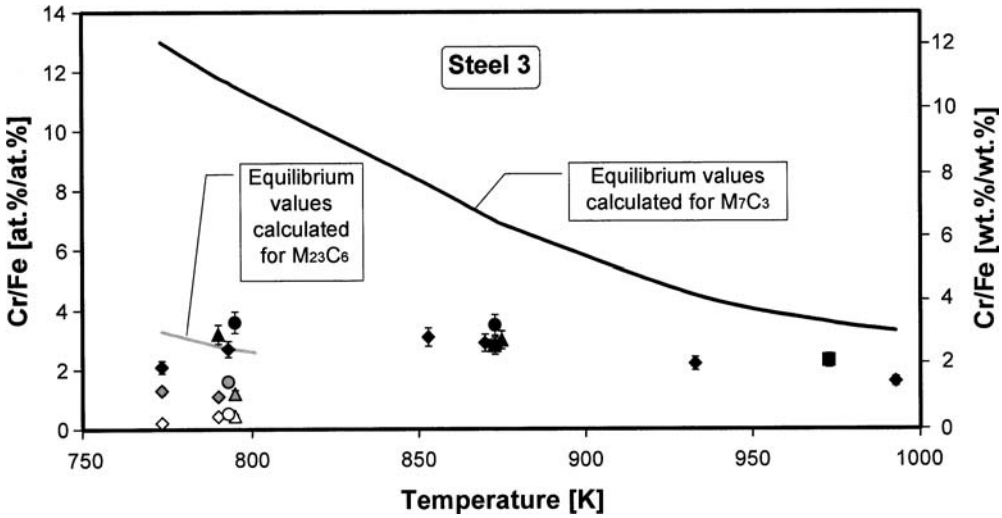

Figure 4 Experimental (points) and calculated equilibrium values (curves) of the Cr/Fe ratio as a function of temperature, plotted for steel 3. Meanings of the non-labelled symbols follow from Table VII.

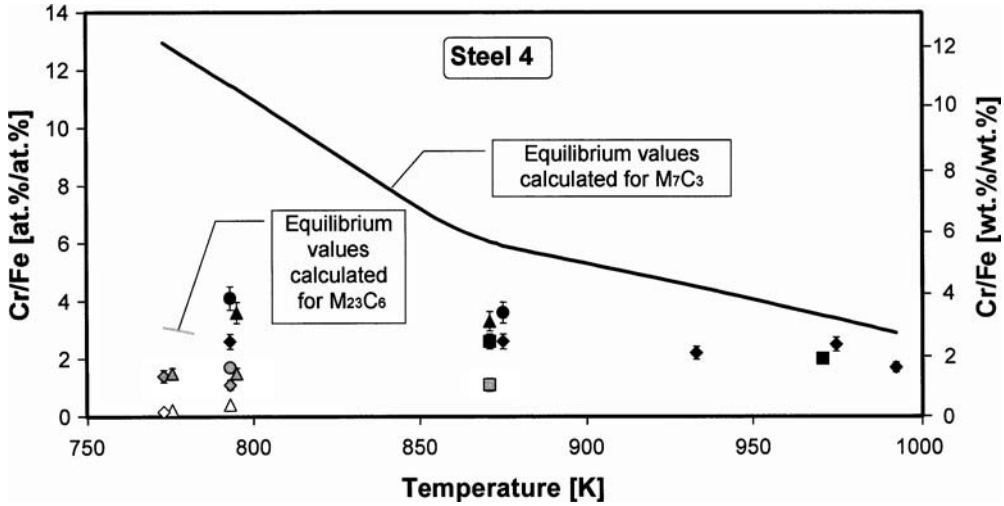

Figure 5 Experimental (points) and calculated equilibrium values (curves) of the Cr/Fe ratio as a function of temperature, plotted for steel 4. Meanings of the non-labelled symbols follow from Table VII.

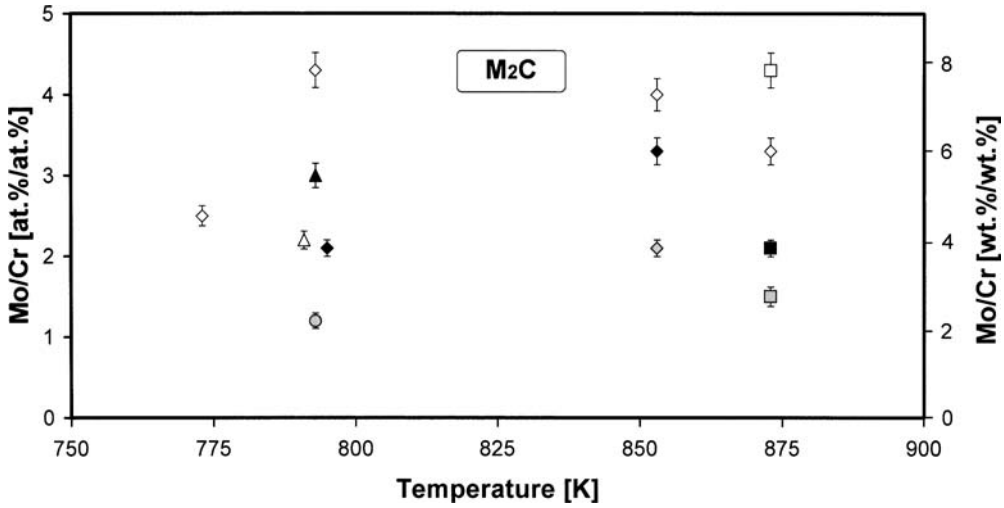

Figure 6 Experimental values (points) of the Mo/Cr ratio as a function of temperature; plotted for M_2C. Meanings of symbols follow from Table VII.

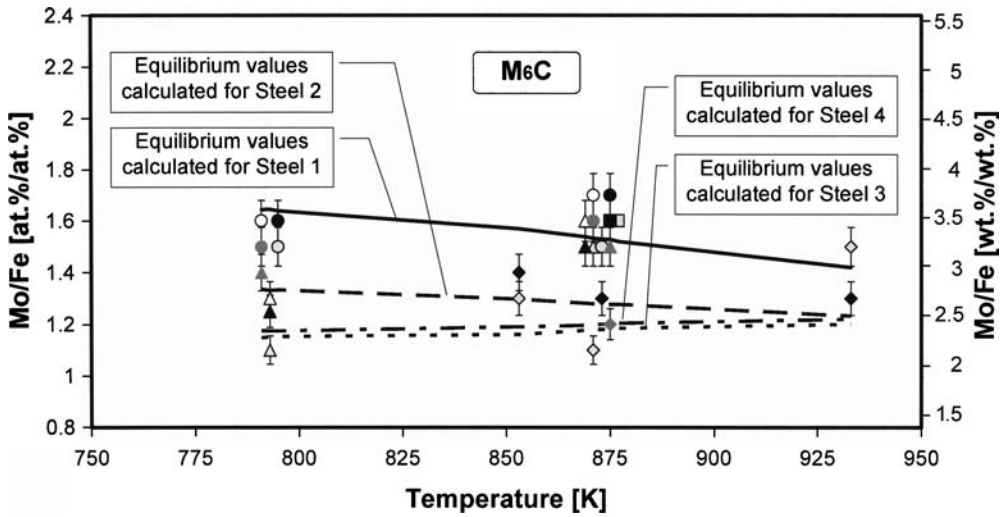

Figure 7 Experimental (points) and calculated equilibrium values (curves) of the Mo/Fe ratio as a function of temperature; plotted for M_6C. Meanings of the non-labelled symbols follow from Table VII.

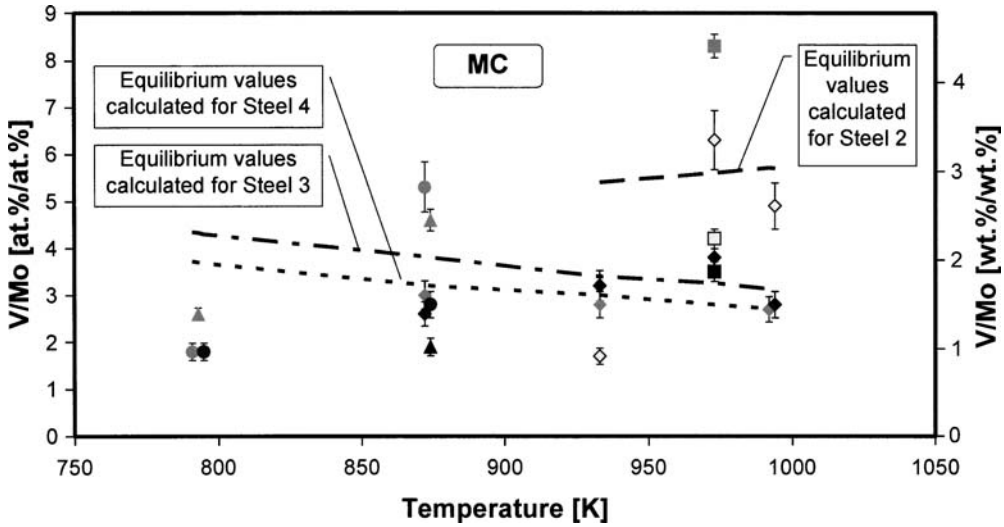

Figure 8 Experimental (points) and calculated equilibrium values (curves) of the V/Mo ratio as a function of temperature; plotted for MC. Meanings of the non-labelled symbols follow from Table VII.

and pressure. Each of the phases considered is modelled as a sum of the reference level of Gibbs energy, entropy term, excess Gibbs energy, and magnetic term (if plausible the magnetic ordering). The thermodynamic parameters were compiled from literature and own assessments, e.g.: [28] (V-N), [29] (Nb-N), [30] (Fe-Cr-Mo), [31] (Fe-Mo-C), [32] (Fe-Nb-C), [33] (Fe-V-C), [34] (Fe-N-C), [35] (Fe-Cr-V), [36] (Fe-Cr-V-C), [37] (Fe-Cr-Ni-C), [38] (Fe-Cr-Mn-N), [39] (Fe-Cr-Mo-N), [40] (Fe-Cr-Ni-C), [41] (Fe-Mo-N-C), [27] (Fe-Cr–Mo–V-C), and [42] (data for pure elements). All elements present in the steels (Table I) were considered in the calculations, except for sulphur and phosphorus which are not included in the database. From phases, ferrite (b.c.c.), austenite (f.c.c.), MC, M_2C, M_3C, M_6C, M_7C_3, and $M_{23}C_6$ were taken into account.

4. Results

Six types of carbides were identified: M_3C, M_2C, M_7C_3, $M_{23}C_6$, M_6C, and MC. In M_3C, M_7C_3, and $M_{23}C_6$ (so-called Fe-Cr-rich carbides), molybdenum, vanadium, manganese, and traces of silicon were found next to iron and chromium. Dominant elements in M_2C were molybdenum, chromium, and vanadium (traces of iron were also identified). In the Mo-Fe-rich M_6C, chromium and vanadium were found next to molybdenum and iron. Vanadium as dominant element was partially substituted with molybdenum and chromium in MC.

The influence of annealing conditions on the occurrence of secondary phases is characterised in Tables II–V. In steel 1, poor in vanadium, all the carbides except for MC were identified (Table II). M_2C was not found in steel 3 (Table IV). In steels 2 (Table III) and 4 (Table V), all the identified carbide types are present in different combinations depending on the temperature and time of annealing. The calculated phase equilibria in the temperature range 750–1000 K are given in Table VI for all the steels. Thermodynamic calculations were done under conditions described in section 3 of this work.

Changes in the Cr/Fe ratio for M_3C, M_7C_3, and $M_{23}C_6$ are plotted in Figs 2–5 in dependence on temperature. Besides points representing the experimental results, curves showing the calculated values for carbides existing in thermodynamic equilibrium at given temperature are also indicated. Meanings of the non-labelled points follow from Table VII. Figs. 2–5 are intended for steels 1, 2, 3, and 4, respectively. The temperature changes in the Mo/Cr ratio are illustrated in Fig. 6 for M_2C. A guide for the assigning experimental points to particular steels and annealing times is available in Table VII. The curves showing equilibrium values are missing, because M_2C was not predicted to be equilibrium phase. In Fig. 7, the experimental (Table VII) and the calculated equilibrium values of the Mo/Fe ratio for M_6C are plotted as a function of temperature. The dependence of the V/Mo ratio on temperature is shown in Fig. 8 for MC. Labelled curves represent the calculated equilibrium values and points (Table VII) are related to the experimental values.

5. Discussion

5.1. The M_3C, M_7C_3, and $M_{23}C_6$

According to the results of the thermodynamic calculations, M_3C is not equilibrium phase, and $M_{23}C_6$ is in equilibrium at lower temperatures only (Table VI). M_7C_3 was predicted to be in equilibrium in wide temperature range for each of the steels. In general, the thermodynamic predictions are in good agreement with the experimental results obtained (compare Tables II–V with Table VI). However, some facts were observed which were not expected originally. For instance, M_3C was identified in steel 2 after longer annealing at 793 K (3000 h) than $M_{23}C_6$ (1000 h), Table III. When compared M_3C and $M_{23}C_6$ in steel 3, the former carbide exists at higher annealing temperatures,

TABLE II. Secondary phases identified in steel 1 annealed at different temperatures (T) for different times (t)

T[K]\t[h]	500	1000	3000	10000
773	–	$M_3C + M_7C_3 + M_{23}C_6 + M_2C$	–	–
793	–	$M_3C + M_7C_3 + M_{23}C_6 + M_2C$	$M_7C_3 + M_2C + M_6C$	$M_7C_3 + M_6C$
853	–	$M_7C_3 + M_{23}C_6 + M_2C$	–	–
873	$M_7C_3 + M_{23}C_6 + M_2C$	$M_7C_3 + M_{23}C_6 + M_2C$	$M_7C_3 + M_6C$	$M_7C_3 + M_6C$
933	–	M_7C_3	–	–
993	M_7C_3	–	–	–

TABLE III. Secondary phases identified in steel 2 annealed at different temperatures (T) for different times (t)

T[K]\t[h]	500	1000	3000	10000
793	–	$M_3C + M_7C_3 + M_{23}C_6$	$M_3C + M_7C_3 + M_6C$	$M_7C_3 + M_2C + M_6C$
853	–	$M_7C_3 + M_{23}C_6 + M_2C + M_6C$	–	–
873	$M_7C_3 + M_{23}C_6 + M_2C + M_6C$	$M_7C_3 + M_{23}C_6 + M_6C$	$M_7C_3 + M_6C$	$M_7C_3 + M_6C$
933	–	$M_7C_3 + MC$	–	–
973	$M_7C_3 + MC$	$M_7C_3 + MC$	–	–
993		$M_7C_3 + M_6C + MC$	–	–

TABLE IV. Secondary phases identified in steel 3 annealed at different temperatures (T) for different times (t)

T[K]\t[h]	500	1000	3000	10000
773	–	$M_3C + M_7C_3 + M_{23}C_6$	–	–
793	–	$M_3C + M_7C_3 + M_{23}C_6$	$M_3C + M_7C_3 + M_{23}C_6 + M_6C$	$M_3C + M_7C_3 + M_{23}C_6 + M_6C$
853	–	$M_3C + M_7C_3$	–	–
873	$M_3C + M_7C_3$	$M_7C_3 + M_6C + MC$	$M_7C_3 + M_6C + MC$	$M_7C_3 + M_6C + MC$
933	–	$M_7C_3 + MC$	–	–
973	$M_7C_3 + MC$	–	–	–
993		$M_7C_3 + MC$	–`	–

TABLE V. Secondary phases identified in steel 4 annealed at different temperatures (T) for different times (t)

T[K]\t[h]	500	1000	3000	10000
773	–	$M_3C + M_{23}C_6$	$M_3C + M_{23}C_6$	–
793	–	$M_3C + M_7C_3 + M_{23}C_6 + M_2C$	$M_7C_3 + M_{23}C_6 + M_2C + M_6C$	$M_7C_3 + M_{23}C_6 + M_6C + MC$
853	–	$M_2C + M_6C$	–	–
873	$M_7C_3 + M_{23}C_6 + M_6C$	$M_7C_3 + M_6C + MC$	$M_7C_3 + M_6C + MC$	$M_7C_3 + M_6C + MC$
933	–	$M_7C_3 + M_6C + MC$	–	–
973	$M_7C_3 + MC$	$M_7C_3 + MC$	–	–
993		$M_7C_3 + MC$	–	–

than the latter carbide (Table IV). In any case, majority of the experimental results has confirmed the sequence of the carbide evolution in Cr–Mo–V low alloy steels proposed earlier [11, 43–46]: $M_3C \rightarrow M_{23}C_6 \rightarrow M_7C_3$. M_7C_3 was identified in nearly all conditions analysed (Tables II–V) that shows an exceptionally high stability of this carbide in the investigated steels and supports the assumption that this carbide is the equilibrium one. Comparison of metal

TABLE VI. Phase equilibria predicted for systems corresponding to he investigated steels; thermodynamic database program ThermoCalc and database Steel16 were used in the predictions

Equilibrium	Steel 1	Steel 2	Steel 3	Steel 4
ferrite + $M_{23}C_6 + M_6C + M_7C_3$	750–779	750–784		
ferrite + $M_{23}C_6 + M_6C + MC$			750–793	750–772
ferrite + $M_6C + M_7C_3$	780–950	785–935		
ferrite + $M_{23}C_6 + M_6C + M_7C_3 + MC$			794–801	773–783
ferrite + M_7C_3	951–1000			
ferrite + $M_6C + M_7C_3 + MC$		936–979	802–961	784–1000
ferrite + $M_7C_3 + MC$		980–1000	962–1000	

Temperature ranges are given in K.

TABLE VII. Meanings of symbols used in Figs 2–8

Annealing time [h]	Appropriate for Figs 2 to 5			Appropriate for Fig. 6 (Mo/Cr for M_2C), Fig. 7 (Mo/Fe for M_6C), and Fig. 8 (V/Mo for MC)			
	M_3C	$M_{23}C_6$	M_7C_3	Steel 1	Steel 2	Steel 3	Steel 4
500	□	□	■	□	□	■	■
1000	◇	◇	◆	◇	◇	◆	◆
3000	△	△	▲	△	△	▲	▲
10000	○	○	●	○	○	●	●

compositions of the carbides (atomic concentrations were taken into account) revealed the following facts: M_3C shows the lowest (between 0.2 and 1), M_7C_3 the highest (between 2 and 5), and $M_{23}C_6$ the medium (between 1 and 2) values of the Cr/Fe ratio (Figs 2–5). An effect of the bulk steel composition on values of the Cr/Fe ratio was not confirmed for any of the carbides.

For M_7C_3, a slight decrease of the Cr/Fe values with increasing temperature was observed, mainly in the temperature range 873–993 K. This is in agreement with both the earlier experimental observations [1, 5, 44, 47–50] and the thermodynamic predictions done (see courses of the black lines in Figs 2–5). For temperatures between 873 and 993 K, a reasonable agreement between the experimental and calculated values was observed. Differences between the experimental and calculated values are evidently bigger in the temperature range 773–873 K. It indicates that annealing at temperatures below 873 K was probably not long enough to reach equilibrium. The time trend of the compositional changes can be assessed at annealing temperatures 793 and/or 873 K, where at least three values of the Cr/Fe ratio per temperature are available. The highest values, as a rule, correspond to the conditions annealed for 10000 h (solid circles in Figs 2–5) that provides evidence about the increase of the Cr/Fe ratio for M_7C_3 with increasing annealing time, regardless of the steel. It is in accordance with the earlier published results [7] and with the tendency to reach the theoretically predicted value as the limiting one.

According to the results of the thermodynamic calculations, $M_{23}C_6$ can be considered as the low-temperature equilibrium carbide. However, $M_{23}C_6$ was also identified at higher annealing temperatures in steels 1, 2, and 4, than are the upper temperature limits of its occurrence in equilibrium (Tables II, III, V, and VI). It suggests either the formation of non-equilibrium $M_{23}C_6$ with the limited microstructure stability at higher temperatures or the need for reassessment of the thermodynamic parameters used in the calculations. The former possibility seems to be more probable. Lack of the experimental data does not allow characterise the compositional evolution of $M_{23}C_6$ and M_3C in detail. However, the Cr/Fe values obtained for the carbides in steels 3 and 4 annealed at 793 K (see the grey-colour and empty symbols in Figs 4–5) provide evidence about both, the compositional stability of M_3C and the increase of the Cr/Fe ratio for $M_{23}C_6$ with increasing the annealing time. When $M_{23}C_6$ and M_7C_3 are compared, the relative chromium contents in the both carbides increase with increasing annealing time. Another common fact for the carbides is the difference between the experimental and the predicted values of the Cr/Fe ratio; the predicted (equilibrium) values are systematically higher, than the experimental ones. Nevertheless the discrepancy between them decreases with increasing time and temperature of annealing, i.e. with nearing the experimental values to equilibrium.

5.2. The M_2C

Between 750 and 1000 K, M_2C was not predicted to be equilibrium phase for any of the steels (Table VI). On the other hand, it was identified experimentally at lower temperatures (773–873 K) and mostly for shorter annealing times (500 and 1000 h) in steels 1, 2, and 4 (Tables II, III, and V). At 793 K, M_2C was also found after longer annealing (for 3000 h in steels 1 and 4; for 10000 h in steel 2). In the latter case, M_2C replaces probably M_3C, present in steel 2 after annealing for 3000 h (Table III). It is difficult to characterise the precipitation behaviour of the unstable M_2C. It can appear in the microstructure after M_6C is already present, as documented for steel 2 annealed at 793 K (Table III). In any case, the long-term stability of M_2C in low alloy steels was observed also earlier. For instance, Foret et al. [49] reported occurrence of M_2C in the 0.17C-1.42Cr-0.92Mo-0.27V steel after 51959 h annealing at 783 K and Kim et al. [51] conceded presence of this carbide in the 0.3C-1.22Cr-0.83Mo-0.22V steel after service at 784 K for 136000 h.

The values of the Mo/Cr ratio for M_2C range between 1 and 5 at.%/at.% (Fig. 6). A limited amount of the experimental results does not give any opportunity to characterise influence of the bulk steel composition and/or the annealing conditions on the Mo/Cr values. With respect to the non-equilibrium character of M_2C, a higher variation in the Mo/Cr values is acceptable. The experimental results revealed that the metal composition of M_2C shows sensitivity to the steel chemical composition, mainly to the bulk Mo/V ratio: the bigger the bulk Mo/V ratio, the bigger the Mo/Cr ratio for M_2C (Fig. 6, Table I).

5.3. The M_6C

The M_6C was predicted to be equilibrium phase for all the steels. Upper limits of the M_6C occurrence in equilibrium range between 950 (steel 1) and over 1000 K (steel 4), Table VI. The predictions are in good agreement with the earlier experimental findings characterising molybdenum as the M_6C stabiliser [46]. It was shown that the annealing for 1000 h at temperatures between 933 and 993 K was not sufficiently long to activate the M_6C precipitation

in all the steels (Tables II–V). On the other hand, M_6C was identified in steel 2 annealed for 1000 h at 993 K (Table III), even if it was predicted to be in equilibrium up to 979 K only (Table VI). This is relatively small difference with respect to the calculation. The clearer answer, concerning the upper temperature existence of this carbide, would need longer annealing times at surrounding temperatures. The kinetic studies at 793 and 873 K (Tables II–V) confirmed that M_6C starts to precipitate after longer annealing times, than M_3C, M_7C_3, M_2C, and $M_{23}C_6$ [45, 52].

Sum of the molybdenum and iron atomic contents represents 80–90% of the M_6C metallic part. This was the reason why the Mo/Fe ratio was chosen to be the criterion for characterisation of compositional changes in M_6C. According to the thermodynamic predictions, the temperature related changes in the Mo/Fe ratio are very small and their course depends on the steel chemical composition (Fig. 7). Thus, the calculated Mo/Fe ratio decreases with increasing temperature for steels 1 and 2. The opposite trend was predicted for steels 3 and 4. The experimental values of the Mo/Fe ratio range between 1.1 and 1.8 at.%/at.%. Even if the values corresponding to 873 K are slightly higher than those corresponding to 793 K, the experimental results do not reveal any clear functional dependence between the Mo/Fe ratio and temperature. The more unambiguous results were obtained from the kinetic studies. The circles corresponding to annealing time 10000 h (Table VII) are positioned in the upper part of the diagram (Fig. 7). It provides evidence about the increase of the Mo/Fe ratio with increasing annealing time. The same result was also presented by Peddle and Pickles [53] for M_6C in the 0.11C-2.06Cr-0.92Mo steel tempered at 811 K, after the post-weld heat treatment done for 3 h at 998 K.

5.4. The MC

MC was not identified experimentally, nor predicted to be equilibrium phase for steel 1 containing 0.02 wt.% of vanadium (Tables II and VI). An increase of the bulk vanadium content to 0.12 wt.% (steel 2) led to the MC stabilisation, but at higher temperatures only (933, 973 and 993 K, Table III). MC was predicted to be in equilibrium at temperatures over 936 K (Table VI) that is in good agreement with the experiment. In steels 3 and 4, which contain the highest amounts of vanadium (Table I), MC was identified in the conditions annealed at higher temperatures as well as in the conditions annealed for longer times at lower temperatures (Tables IV and V). According to the thermodynamic predictions, MC in steels 3 and 4 is equilibrium phase in the whole temperature range considered (750–1000 K). The above presented findings revealed:

- MC starts to precipitate after longer periods of annealing than the Fe-Cr-rich carbides (M_3C, M_7C_3, and $M_{23}C_6$): the lower the annealing temperature, the longer the period needed for starting precipitation.
- Good agreement was achieved between the experimental results and the thermodynamic predictions.

The experimentally obtained values of the V/Mo ratio for MC range between 1 and 6.5 at.%/at.% (Fig. 8), except for the value 8.3 at.%/at.% corresponding to steel 3 annealed for 500 h at 873 K. The anomalous value can be attributed to the higher chemical heterogeneity of the sample. Otherwise, the differences between V/Mo values are not great, even though the analysed particles precipitated probably in different stages of annealing and differ from each other in sizes and shapes.

It was shown earlier that the higher bulk vanadium content promotes a dominance of vanadium in MX in Cr-V low alloy steels [50]. The similar tendency for the bulk molybdenum content was observed in this work. Steels 3 and 4 have practically identical chemical compositions, except for the molybdenum content (Table I). It was found out that the relative amounts of molybdenum in MC (compare values of the V/Mo ratio in Fig. 8) are systematically higher for steel 4 with the higher bulk molybdenum content (compared to steel 3). It is well noticeable at the lower annealing temperatures mainly. Lack of the experimental data does not make possible to comment changes in values of the V/Mo ratio for MC in dependence on the annealing time. However, the results obtained for temperature 873 K (Fig. 8) revealed that MC contains more vanadium (related to the molybdenum content) when steels 3 and/or 4 are annealed for longer periods. This is in agreement with the scheme published in work [5], where the time-dependent changes in M/Mo ratios (M = V, Cr or V + Cr) for different carbides present in low alloy steels are illustrated. It was shown that the M/Mo values decrease with increasing time in the initial period of annealing. Then, the M/Mo values grow up until the saturation under near-equilibrium conditions is reached. It was also stated that position of the minimum in the kinetic dependence of the M/Mo values is a function of annealing temperature: the higher the annealing temperature, the shorter the time needed for reaching minimum. The annealing times used in this work (between 1000 and 10000 h, Fig. 8) correspond evidently to the growing up part of the kinetic dependence presented in the work [5].

5.5. General remarks on carbide evolution

Low alloy steels have been employed in energy industries as components of power boilers (waterwall, superheater) over 50 years. For instance, the classical 2,25Cr-1Mo steel has been used worldwide in high capacity power stations with excellent operating behaviour. The effort to increase steam parameters and service efficiency of new boilers calls for materials with a higher microstructure stability and better creep properties.

In this work, the experimental and calculated data are given making possible evaluation and/or prediction

of changes in metal compositions of carbides during long-term service. Even if the diagrams (Figs 2–8) were constructed for four steels only, some of the documented tendencies (e.g. changes of the values of concentration ratios for individual carbides in dependence on annealing temperature and/or time) are of general validity.

6. Conclusions

The low alloy steels with different contents of molybdenum and vanadium, marked as 1, 2, 3, and 4, were investigated with the use of TEM and thermodynamic calculations. The steels were annealed at 773, 793, 853, 873, 933, 973, and 993 K for 500, 1000, 3000, and 10000 h. The results obtained can be summarised as follows:

- Carbides M_3C, M_2C, M_7C_3, $M_{23}C_6$, M_6C, and MC were identified in steels 2 and 4. The same carbides except for MC and M_2C were found in steels 1 and 3, respectively.
- It was confirmed validity of the earlier proposed sequence of carbide evolution: $M_3C \rightarrow M_{23}C_6 \rightarrow M_7C_3$. The $M_{23}C_6$ was considered as equilibrium carbide existing at lower temperatures.
- Carbides M_6C and MC were found to start to precipitate after longer annealing times in comparison to carbides M_3C, M_7C_3, and $M_{23}C_6$.
- The experimental values of Cr/Fe ratio [at.%/at.%] range between 0.2 and 1 for M_3C, between 1 and 2 for $M_{23}C_6$, and between 2 and 5 for M_7C_3, regardless of the bulk steel composition.
- It was found out that the bulk Mo/V ratio affects the metal composition of M_2C: the bigger the bulk Mo/V ratio, the bigger the Mo/Cr ratio for M_2C.
- The bulk molybdenum content was found to influence the metal composition of MC: the bigger the bulk molybdenum content, the lower the V/Mo ratio for MC.
- It was achieved good agreement between the experimental and the thermodynamically predicted data.

References

1. J. JANOVEC, in Nature of Alloy Steel Intergranular Embrittlement (Veda, Bratislava, 1999) p. 76.
2. J. H. WOODHEAD and A. G. QUARRELL, *JISI* **203** (1965) 605.
3. K. H. KUO and C. L. JIA, *Acta Mater.* **33** (1985) 991.
4. H. K. D. H. BHADESHIA and J. W. CHRISTIAN, *Metal. Trans.* **21A** (1990) 767.
5. J. JANOVEC, A. VÝROSTKOVÁ and A. HOLÝ, *J. Mater. Sci.* **27** (1992) 6564.
6. K. W. ANDREWS, H. HUGHES and D. J. DYSON, *JISI* **210** (1972) 337.
7. R. C. THOMSON and H. K. D. H. BHADESHIA, *Mater. Sci. Technol.* **10** (1994) 193.
8. R. C. THOMSON and H. K. D. H. BHADESHIA, *Mater. Sci. Technol.* **10** (1994) 205.
9. V. VODÁREK and A. STRANG, *Scripta Mater.* **38** (1998) 101.
10. V. VODÁREK and A. STRANG, *Mater. Sci. Technol.* **16** (2000) 1207.
11. B. A. SENIOR, *Mater. Sci. Engn.* **A103** (1988) 263.
12. V. VODÁREK, J. SOBOTKA and M. SOBOTKOVÁ, *Z. Metallkde.* **82** (1991) 22.
13. D. V. SHTANSKY and G. INDEN, *Acta Mater.* **45** (1997) 2861.
14. S. JONSSON, *Z. Metallkde.* **87** (1996) 703.
15. H. J. GOLDSCHNIDT, *JISI* **160** (1948) 345.
16. K. KUO, *JISI* **173** (1953) 363.
17. E. KOZESCHNIK and J. M. VITEK, *Calphad* **24** (2000) 495.
18. A. GÜTH, A. KAUN, A. KÖTHE, D. MÜLLER and J. RICHTER, *J. Scripta Metall.* **21** (1987) 163.
19. R. C. THOMSON and M. K. MILLER, *Acta Mater.* **46** (1998) 2203.
20. V. SLUGEŇ, *Mössbauer Spectr. Mater. Sci.* **66** (1999) 119.
21. P. STRUNZ, J. ZRNÍK, A. GILLES and A. WIEDERMANN, *Physica B* **276–278** (2000) 890.
22. G. D. PIGROVA, *Metall. Mater. Trans.* **27A** (1996) 498.
23. M. HILLERT and L. I. STAFFANSSON, *Acta Chem. Scand.* **24** (1970) 3618.
24. B. SUNDMAN, in Thermo-Calc, version L (Royal Inst. Tech., Stockholm, 1997) p. 1.
25. R. H. DAVIES, A. T. DINSDALE, T. G. CHART, T. I. BARRY and M. H. RAND, *High Temperature Sci.* **26** (1990) 251.
26. A. BJÄRBO and M. HÄTTESTRAND, *Metall. Mater. Trans.* **31A** (2000) 1.
27. A. KROUPA, J. HAVRÁNKOÁ, M. COUFALOVÁ, M. SVOBODA and J. VŘEŠŤÁL, *J. Phase Equi.* **22** (2001) 312.
28. Y. DU, R. SCHMID-FETZER and H. OHTANI, *Z. Metallkde.* **88** (1997) 545.
29. W. HUANG, *Metall. Mater. Trans.* **27A** (1996) 3591.
30. J. O. ANDERSON and N. LANGE, *Metall. Mater. Trans.* **19A** (1988) 1385.
31. J. O. ANDERSON, *Calphad* **12** (1988) 9.
32. W. HUANG, *Z. Metallkde.* **81** (1990) 397.
33. W. HUANG, *Z. Metallkde.* **82** (1991) 391.
34. H. DU and M. HILERT, *Z. Metallkde.* **82** (1991) 310.
35. B. J. LEE, *Z. Metallkde.* **83** (1992) 292.
36. B. J. LEE and D. N. LEE, *J. Phase Equi.* **13** (1992) 349.
37. M. HILERT and C. QIU, *Metall. Trans.* **23A** (1992) 1593.
38. C. QIU, *Metall. Trans.* **24A** (1993) 2393.
39. K. FRISK, *Calphad* **15** (1991) 79.
40. B. J. LEE, *Calphad* **16** (1992) 121.
41. K. FRISK and B. URHENIUS, *Metall. Mater. Trans.* **27A** (1996) 2869.
42. A. T. DINSDALE, *Calphad* **15** (1991) 317.
43. R. SMITH, *ISI Special Report* **64** (1959) 307.
44. J. JANOVEC, A. VÝROSTKOVÁ and M. SVOBODA, *Metall. Mater. Trans.* **25A** (1994) 267.
45. A. VÝROSTKOVÁ, A. KROUPA, J. JANOVEC and M. SVOBODA, *Acta Mater.* **46** (1998) 31.
46. A. KROUPA, A. VÝROSTKOVÁ, M. SVOBODA and J. JANOVEC, *Acta Mater.* **46** (1998) 39.
47. R. PETRI, E. SCHNABEL and P. SCHWAAB, *Arch. Eisenhüttenwes.* **52** (1981) 71.
48. J. JANOVEC, V. MAGULA, A. HOLÝ and A. VÝROSTKOVÁ, *Scripta Metall. Mater.* **26** (1992) 1303.
49. R. FORET, J. KRUMPOS, J. SOPOUŠEK, M. SVOBODA and J. VŘEŠŤÁL, *Z. Metallkd.* **92** (2001) 307.
50. J. JANOVEC, A. VÝROSTKOVÁ, M. SVOBODA, A. KROUPA and H. J. GRABKE, *Metall. Mater. Trans.* **35A** (2004) 751.
51. S. KIM, A. SHEKHTER and S. P. RINGER, *Int. J. Pressure Vessel Piping* **79** (2002) 571.
52. J. PILLING and N. RIDLEY, *Metall. Trans.* **13A** (1982) 557.
53. B. E. PEDDLE and C. A. PICKLES, *Canad. Metall. Quart.* **40** (2001) 105.

Received 23 May
and accepted 29 August 2005